ORNL/TM-2024/3336
CRADA/NFE-20-08315

CRADA Final Report: CRADA Number NFE-20-08315 with Reactwell L.L.C.

Radu Custelcean
Costas Tsouris
Brandon Iglesias

Date: March 25, 2024

OAK RIDGE NATIONAL LABORATORY
MANAGED BY UT-BATTELLE FOR THE US DEPARTMENT OF ENERGY

ORNL/TM-2024/3336
CRADA/ NFE-20-08315

CRADA Final Report: CRADA Number NFE-20-08315 with Reactwell L.L.C.

Integrated Process for Direct Air Capture of CO_2 and Electrochemical Conversion to Ethanol

Radu Custelcean, PI (ORNL)
Costas Tsouris, co-PI (ORNL)
Brandon Iglesias, participant (Reactwell)

Date Published:
March 25, 2024

Prepared by
OAK RIDGE NATIONAL LABORATORY
Oak Ridge, Tennessee 37831-6283
managed by
UT-BATTELLE, LLC
for the
US DEPARTMENT OF ENERGY
under contract DE-AC05-00OR22725

1. Abstract

This Cooperative Research and Development Agreement (CRADA) between UT-Battelle, LLC and Reactwell, L.L.C. aimed to facilitate the development of an energy-efficient and cost-effective technology that captures carbon dioxide (CO_2) from ambient air and converts it electrochemically to ethanol. Direct air capture (DAC) of CO_2 offers the prospect of permanently lowering the atmospheric CO_2 concentration, providing economic and energy-efficient technologies can be developed and deployed at a large scale. DAC has the potential for high-capacity atmospheric CO_2 capture, the flexibility of placement anywhere on earth, and the generation of high-purity CO_2 streams. The most significant technical challenge with DAC is the very low atmospheric concentration of CO_2, thereby requiring sorbents that bind CO_2 quickly, strongly, and selectively against other components in the air. Integrating DAC with CO_2 conversion into useful chemicals, fuels, or materials can provide an economically feasible solution for mitigating climate change. As long as the carbon contained in these products is taken from the atmosphere and no additional carbon emissions result from their production, processing, and transportation, they can be considered carbon-neutral products. This CRADA facilitated the development of a new net-zero emission technology that closes the carbon cycle by combining DAC with the catalytic electrochemical conversion of CO_2 into ethanol.

2. Statement of Objectives

This CRADA had the following objectives:

1. **Optimization of DAC Chemistry**
   The goal of this task was to identify the optimal amino acid/guanidine combinations and reaction conditions that maximize the rate of CO_2 absorption and the amount of CO_2 removed from air in the DAC process. The influence of the various crystallization parameters was evaluated to identify the conditions leading to the most efficient CO_2 separation.
2. **Contactor Design, Manufacturing and Testing**
   The air–liquid contactor is a critical part of the DAC system, and it should ensure fast mass transfer of CO_2 from air into the aqueous solution, and minimal sorbent loss and environmental contamination. Two major objectives under this task were to (*i*) expedite the absorption process and (*ii*) make the device highly compact so that it takes minimum footprint and energy and can be easily integrated into the overall process.
3. **Optimization of Sorbent Regeneration and CO_2 Release**
   In this task we optimized the CO_2 release step with the goals to improve heat transfer, minimize the energy consumption, and maximize the purity and pressure of the CO_2 needed for efficient conversion to ethanol. Moreover, we explored the possibility of using renewable energy sources, low-grade waste heat, or high-temperature heat pumps for the CO_2 release.
4. **DAC Process Engineering and Intensification**
   In this task, a continuous intensified DAC process that combines two or more operations into a single step was demonstrated. Specifically, we combined CO_2 absorption by amino acid and crystallization with the guanidine compound. Packed and spray column designs

were initially employed for this purpose and were subsequently replaced by the improved air–liquid contactor developed in Task 2.

5. **Atmospheric Water Capture**
   The goal of this task was to integrate an atmospheric water capture (AWC) unit into the DAC process to compensate for the water loss during the CO_2 absorption toward an environmentally sustainable DAC technology. The AWC unit offers the prospect for integration into the DAC process, by placing it down the line from the air–liquid contactor, thereby recycling the recovered water back into the contactor.
6. **Electrochemical Conversion of CO_2 to Ethanol**
   This task aimed to improve the electrochemical conversion of carbon dioxide to ethanol and integrate it with the DAC process. The efforts were focused on three lines of development: (1) catalyst prototyping based on carbon nanospike/copper nanoparticles, (2) electrochemical reactor cells and cell stack, and (3) potentiostat controls and power systems. Another part of this task was to engineer a process that collects the captured CO_2 and deliver it straight into the electrochemical reactor. Alternatively, we considered the feasibility of directly reducing the aqueous (bi)carbonate anions resulting from the capture process into ethanol, to bypass the energy-intensive CO_2 release step.
7. **Technoeconomic and Lifecycle Analyses**
   Technoeconomic assessment (TEA) was performed as part of this task to evaluate the DAC process in terms of cost per net unit mass of CO_2 removed from the atmosphere. Furthermore, a holistic Lifecycle (LC) analysis remains to be performed to determine the environmental burden (or benefit) of the DAC process.
8. **Technology Scale-up and Commercialization**
   We proposed a three-step technology development plan: Step 1 – demonstrate a bench-scale DAC system operating at steady state; Step 2 – integrate DAC system with carbon dioxide electrochemical conversion to ethanol conversion system; Step 3 – produce ethanol from captured carbon dioxide via natural amino acid and sell high margin, low volume (750 ml to 1000 ml) of vodka spirits. A modular system was proposed to be built, integrating the DAC and electrochemical ethanol production within a twenty-foot or forty-foot cargo container, to enable field deployment in a ruggedized form factor.
9. **Final Report**
   A final report summarizing all the project achievements to be written and distributed to the sponsor and the interested parties.

3. Benefits to the Funding DOE Office Mission

The R&D under this CRADA was expected to lead to new and improved technologies for carbon capture and conversion to fuels (e.g., ethanol). As such, it would benefit the DOE mission for clean energy, energy security, environmental stewardship, and climate change mitigation.

4. Technical Discussion of Work Performed by All Parties

4.1. Optimization of DAC Chemistry

The main goal of this task was to identify the optimal amino acid/guanidine combinations and reaction conditions that maximize the rate of CO_2 absorption and the amount of the CO_2 removed from air. The guanidine was selected from a series of bis-iminoguanidines (BIGs) previously studied at ORNL.[1-3] One particularly promising BIG recently developed in our labs is methylglyoxal-bis(iminoguanidine) (MGBIG).[4] Its aqueous solubility of about 1 mol/L is significantly higher compared to analogous BIGs, which allows us to employ MGBIG as an aqueous solvent in a DAC process, an option not available with the less soluble BIG analogs. In the presence of atmospheric CO_2, MGBIG forms two main crystalline carbonate structures depending on the initial concentration of MGBIG. At concentrations greater than 0.75 mol/L, MGBIG crystallizes primarily as $(MGBIGH^{+})_2(CO_3^{2-})(H_2O)_2$, or phase 1 (P1). At concentrations lower than 0.3 mol/L, MGBIG crystallizes mostly as $(MGBIGH_2^{2+})(CO_3^{2-})(H_2O)_2$, or phase 3 (P3). Variable mixtures of the two phases are usually formed from solutions of intermediate concentrations. The main difference between the two phases is the degree of MGBIG protonation – mono-protonated in P1 and di-protonated in P3, as determined by single-crystal neutron diffraction. From an atom economy perspective, P3 is preferred over P1, as only one equivalent of MGBIG is needed for the former, compared to two equivalents of MGBIG for the latter, for each equivalent of CO_2 captured. While thermodynamically favorable and driven by the very low aqueous solubility of the MGBIG carbonate salt, the overall DAC process is very slow, restricted by the diffusion of the CO_2 from air into the solution, and the limited alkalinity of the BIG solution.

Addition of an amino acid to the MGBIG solution was found to significantly accelerate the rate of CO_2 absorption and increase the total amount of the CO_2 removed from air.[5] The effects of various amino acids and oligopeptides, such as glycine, sarcosine, serine, arginine, taurine, lysine, and glycylglycine, on the efficacy of DAC by crystallization of MGBIG carbonate were initially investigated. While most of the amino acids studied were found to precipitate with MGBIG, thereby rendering the sorbent unavailable for DAC, sarcosine (SAR), the only amino acid in the series with a secondary amine group, remained soluble in the presence of MGBIG, leading to enhanced DAC compared to MGBIG alone. While in the previously studied systems the DAC process comprised CO_2 absorption with aqueous amino acid salts (amino acid + KOH) in a first step, followed by (bi)carbonate crystallization with solid BIGs in a subsequent step, in the current system, the high aqueous solubility of MGBIG allows for the two reactions to be combined into an intensified process. Another advantage of combining amino acids and MGBIG solutions is that the guanidine groups can act as bases that deprotonate and activate the amino groups for reaction with CO_2, thereby circumventing the need to use KOH base.

In the next set of DAC experiments, we investigated the effect of SAR concentration on the MGBIG carbonate crystallization yield and the crystalline phase formed. Keeping the initial concentration of MGBIG to 0.5 M, the concentration of SAR was varied from 0 to 0.5 M. The observed yields of crystallization, measured as the mol% of MGBIG removed from solution after two weeks of exposure to open air, are plotted in Figure 1. The phase identities of the crystallized solids were determined by optical microscopy and X-ray diffraction. P1 and P3 of MGBIG-CO_3 have very different morphologies, prisms and needles, respectively, making the differentiation straightforward by optical microscopy. These phases were additionally confirmed by single-crystal

X-ray diffraction. In the absence of SAR, P1 MGBIG-CO_3 crystallized in 28% yield. On the other hand, only 0.05 M SAR was sufficient to induce a switch to P3 MGBIG-CO_3, and a significant boost in the crystallization yield to 83%. The yield of MGBIG-CO_3 P3 crystallization remained virtually constant up to 0.3 M MGBIG, and then it slightly declined at 0.4 and 0.5 M MGBIG concentrations. The addition of a small amount of SAR to the aqueous MGBIG solvent–as little as 0.5 mmol–led to extraction of six times as much CO_2 from the air (4.15 mmol vs. 0.7 mmol). Thus, aqueous MGBIG and sarcosine work in synergy, offering the prospect for an effective DAC process.

To scale up the DAC chemistry, we employed an Envion air humidifier serving as an air–liquid contactor (Figure 1).

Figure 1. DAC setup using an Envion air humidifier as an air–liquid contactor.

Screening DAC tests were done to determine the optimal concentrations of MGBIG and SAR that maximize the yield of crystallization, the proportion of P3, and the amount of CO_2 removed from air. All DAC measurements were run for 24 h with 1 L solution of variable MGBIG and SAR concentrations using the humidifier as an air–liquid contactor (Figure 1). The extents of the DAC reactions were monitored *in situ* by pH measurements, and *ex situ* by periodically withdrawing samples and measuring the total amount of CO_2 absorbed by Total Inorganic Carbonate (TIC) analysis, and the amount of MGBIG crystallized out of solution by quantitative ^{1}H NMR spectroscopy. The results are summarized in Table 1, and typical evolutions of the pH and the [MGBIG] and [SAR] concentrations as functions of time are shown in Figure 3. Sarcosine was found to have a dramatic influence over the yield of crystallization and the identity and phase composition of the crystals formed. Without any SAR present, the crystallization yield from a 0.5 M MGBIG solution was very low (14%), and little or no carbonate crystals formed after 24 h of DAC, based on TIC and elemental analyses of the isolated solid. Adding even a small amount of SAR (0.1 mol/L) dramatically increased the yield of MGBIG crystallization (77%), as an almost equimolar mixture of P1 and P3. Increasing the concentration of SAR to 0.2 mol/L maintained a

high crystallization yield (64%), and P3 became the dominant phase formed after 24 h (up to 74 mol%). The proportion of P3 grew further to 83 mol% when the concentration of SAR was increased to 0.3 mol/L, while the yield of crystallization remained relatively high at 59%. Maintaining the concentration of SAR to 0.3 mol/L and decreasing the initial concentration of MGBIG from 0.5 to 0.3 mol/L led to a similar crystallization yield, but the phase formed was almost exclusively P3. Finally, increasing the concentrations of MGBIG and SAR to 0.7 and 0.4 mol/L, respectively, maintained a high crystallization yield, though the major phase became P1. Thus, from these screening experiments, the optimal concentrations of MGBIG and SAR that maximize the crystallization yield and the proportion of P3 appear to be 0.3-0.5 M and 0.3 M, respectively. Under these conditions, the solution pH dropped significantly for the first 8 h, then it plateaued around 9.9, while the concentration of MGBIG decreased monotonously throughout the DAC experiment (Figure 2). On the other hand, based on the quantitative NMR measurements, virtually no SAR was removed from solution.

Table 1. Screening RC-DAC experiments with various initial MGBIG and SAR concentrations.

[MGBIG] mol/L	**[SAR]** mol/L	**pH initial**	**pH final**	**MGBIG crystallization yield**[a] %	**P1**[b] mol%	**P3**[b] mol%
0.5	0	12.12	11.24	14	NA	NA
0.5	0.1	10.30	9.67	77	54-67	46-33
0.5	0.2	10.50	10.09	64	26-37	74-63
0.5	0.3	10.20	9.91	59 ± 8[c]	17 ± 16[c]	83 ± 16[c]
0.3	0.3	10.17	9.81	59	1	99
0.7	0.4	10.5	10.08	61	65	35

[a]From the concentration of MGBIG left in solution determined by quantitative NMR; [b]From a combination of elemental analysis and TIC; [c]Average values from 4 separate experiments.

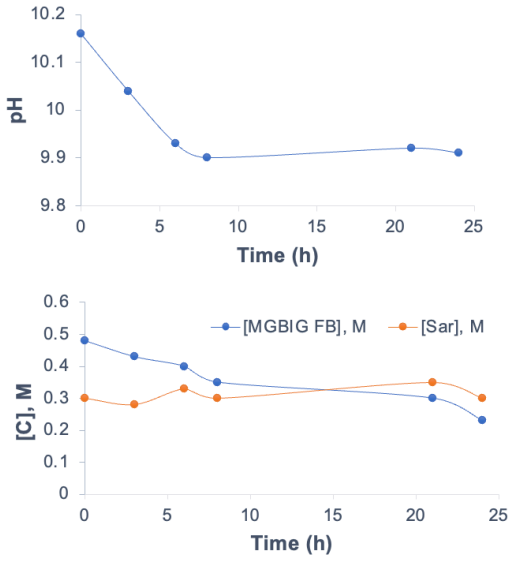

Figure 2. Monitoring the evolutions of pH (top), and of the concentrations of MGBIG free base (FB) and SAR as functions of time, as determined by quantitative ^{1}H NMR spectroscopy. Initial concentrations: [MGBIG] = 0.5 M; [SAR] = 0.3 M.

Having identified the optimal concentrations of MGBIG (0.5 M) and SAR (0.3 M) that maximize the yield of crystallization, the proportion of P3, and the amount of CO_2 removed from air, in the next phase we tested the robustness of the DAC process with MGBIG/SAR over consecutive DAC cycles. We ran a total of 10 cycles, each cycle consisting of CO_2 uptake from air for 24 h with the humidifier, removal of the MGBIG carbonate crystals from the resulting slurry by vacuum filtration, drying the crystals in air, then releasing the CO_2 and regenerating MGBIG by heating the carbonate crystals at 140 °C in the oven. The SAR filtrate and the regenerated MGBIG solid were then recycled into the humidifier. The results from MGBIG carbonate crystallization with the humidifier for the 10 cycles are depicted in Figure 3. The average yield of carbonate crystallization was 51% ± 10%, with 91 ± 13 mol% P3 observed. This corresponds to a cyclic capacity of 0.23 ± 0.02 mol CO_2/L, or 10 ± 1 g CO_2 removed from air per 24 h cycle.

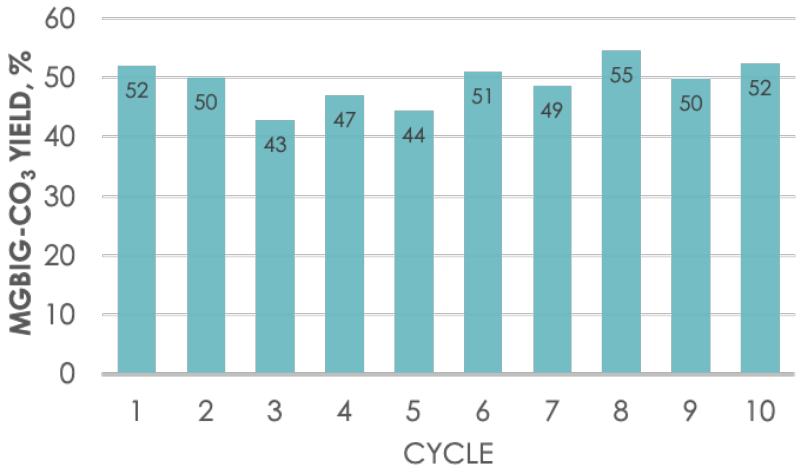

Figure 3. MGBIG-CO_3 crystallization yields measured for 10 consecutive DAC cycles run with 0.5 M MGBIG and 0.3 M SAR in the humidifier.

Once the DAC chemistry was optimized, our focus shifted to the design, manufacturing, and testing of an improved air–liquid contactor with larger surface area for faster DAC at a larger scale.

4.2. Contactor Design, Manufacturing and Testing

While the humidifier proved useful for optimizing the DAC chemistry, to scale up our DAC process we needed a larger air–liquid contactor with enhanced surface area. However, we wanted to keep the basic design behind the humidifier, as we found it can handle solid-liquid slurries very well. We refer to this design as a Rotating Air Contactor, or RAC. Unlike in the typical air–liquid DAC contactor, in which the contactor itself is stationary and the liquid moves over it with the help of a pump, in RAC the liquid is largely stationary but the contactor itself (its fabric, more precisely) rotates through the solvent, with the help of a motor and a rotor, to spread the solvent over its surface and expose it to air for DAC. Starting from the humidifier as our starting point, we designed the RAC with an enhanced air–liquid contact area by multiplying the number of rotors so it can accommodate a longer fabric that provides a larger surface area (Figure 4). While in the prototype we maintained the same width for the fabric, increasing the fabric's width is an obvious way to scale up and further increase the surface area in future generations RACs. Our prototype RAC (Figure 5) had an estimated air–liquid contact area, corresponding to the surface of the fabric exposed to air, of about 0.5 m^2, which is about twice as large as that of the humidifier.

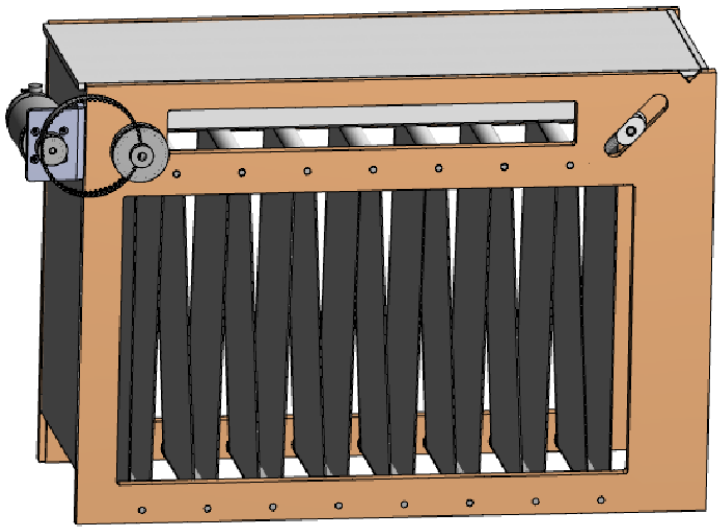

Figure 4. Rotating Air Contactor (RAC) design.

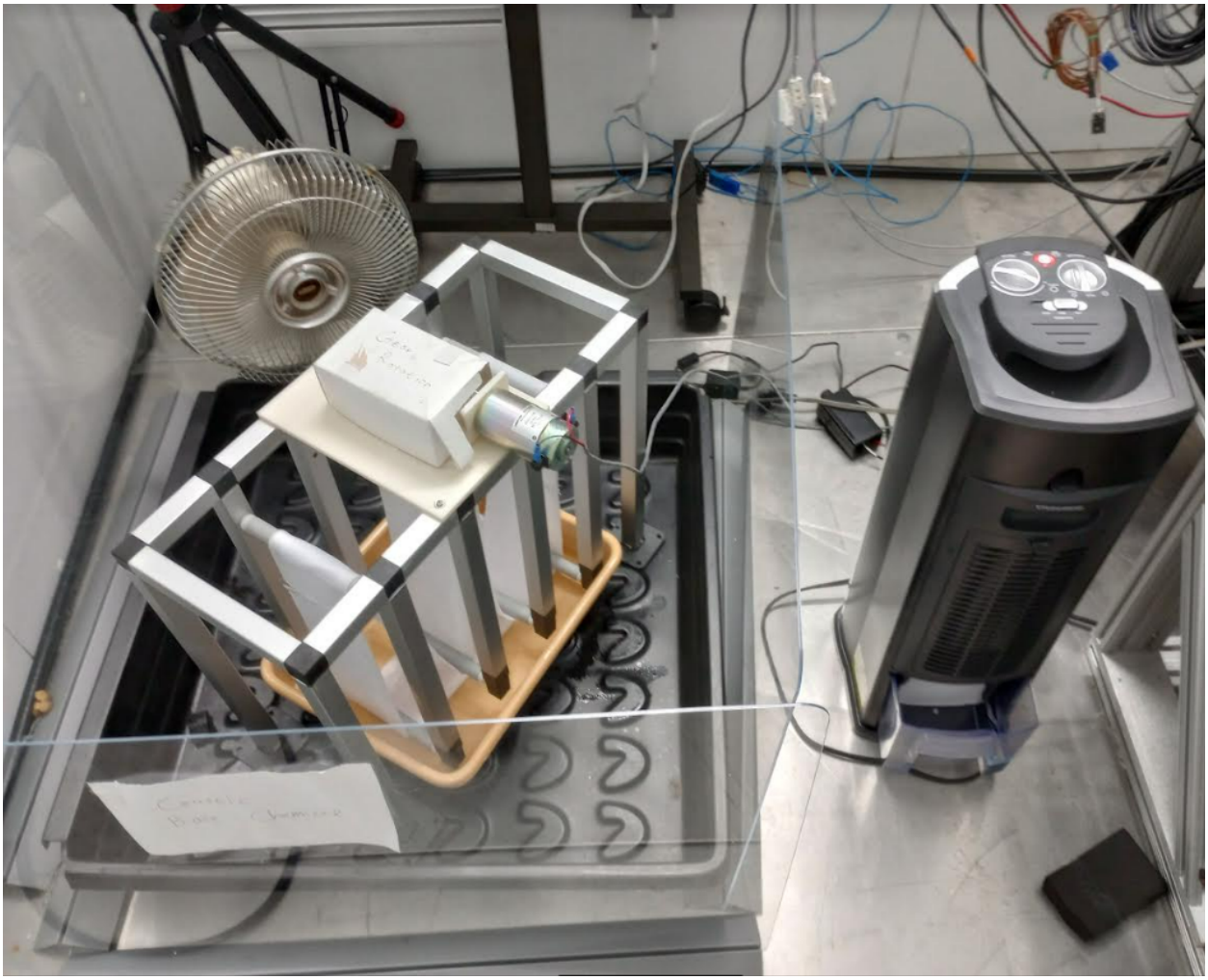

Figure 5. Prototype RAC shown side by side with the humidifier.

We tested our prototype RAC using a 2 L solution of 1 M K-SAR (no guanidine). Two DAC CO_2 loading tests were initially done inside a climate-controlled room, at 35 and 65 F, and 80% relative humidity (RH). As shown in Figure 6, the RAC significantly outperforms the humidifier in both experiments.

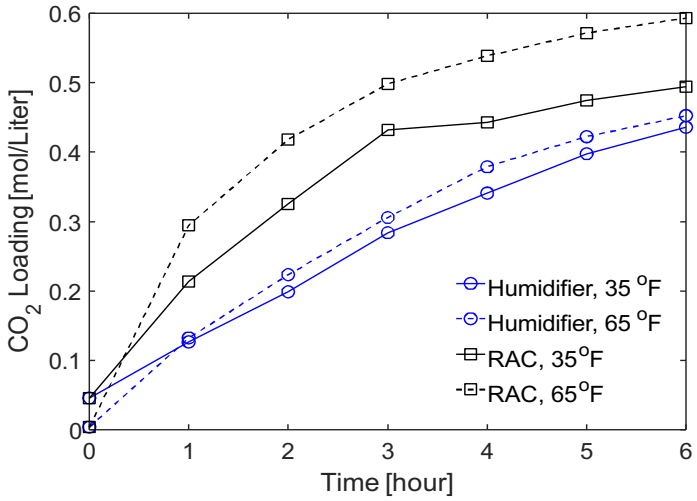

Figure 6. Atmospheric CO_2 loading with the prototype RAC in comparison with the humidifier. The DAC tests were done with 2 L of K-SAR (1 M) in a climate-controlled room set at 35 and 65 °F, and 80% RH.

In a following DAC test, we loaded the RAC with 2 L solvent containing SAR (0.3 M) and MGBIG (0.5 M), a solvent composition previously optimized using the humidifier. The test was run side by side with the humidifier loaded with 1 L of the same solvent. Both experiments were run at 25 °C and 70% RH. After 24 h, the yield of MGBIG-CO_3 crystallization in both contactors was similar, around 60-62%, but the amount of isolated carbonate solids and CO_2 removed was almost 3 times larger with the RAC (22 g) compared to that from the humidifier (8.3 g).

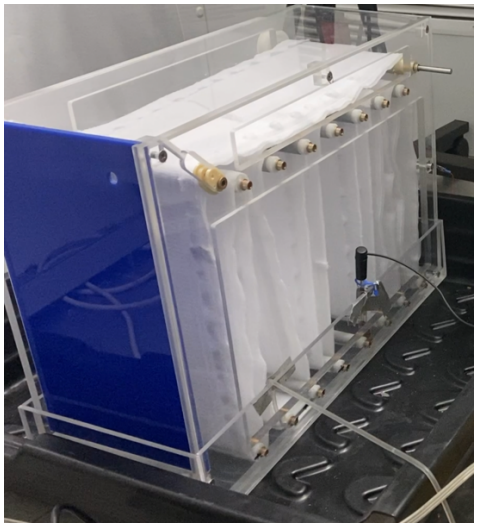

Figure 7. 2nd gen RAC, with an estimated air–liquid contact area of 1.2 m^2.

The second-generation RAC was then built, further increasing the number of rotors and the length of the fabric, which led to an estimated air–liquid contact area of 1.2 m^2 (Figure 7). The initial tests with 1 M K-SAR showed the 2nd gen RAC had a CO_2 uptake rate from the air about twice as high than the prototype RAC (Figure 8).

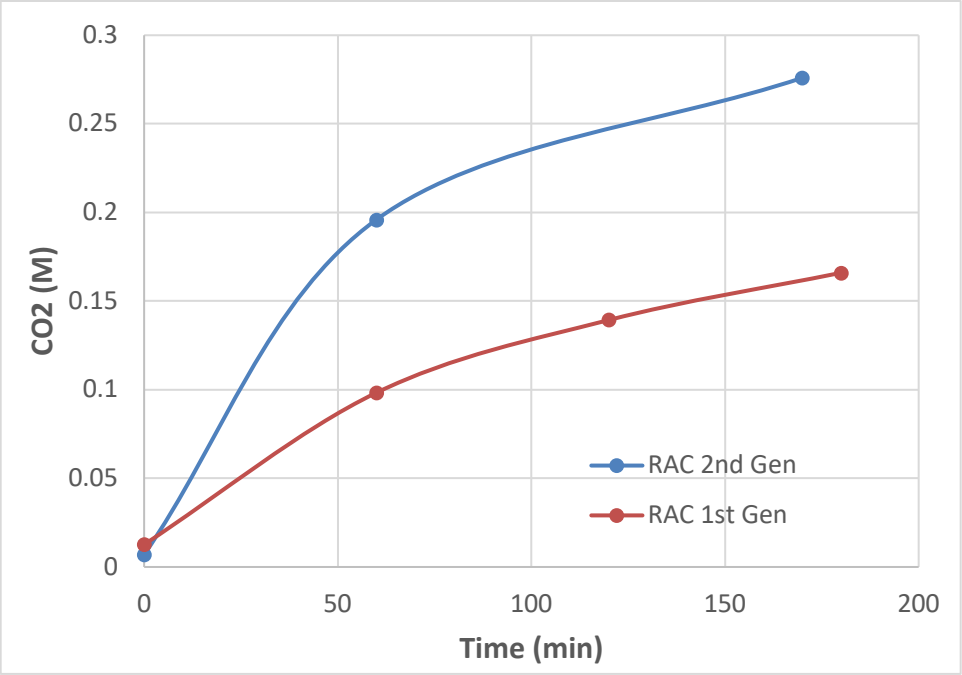

Figure 8. Comparison of atmospheric CO_2 loading (65 F, 80% RH) with 1st and 2nd gen RACs, using 1 M K-SAR.

These tests demonstrated that the initial rates of atmospheric CO_2 capture with 1 M aqueous K-SAR increase proportionally with the available air–liquid contact area (Figure 9).

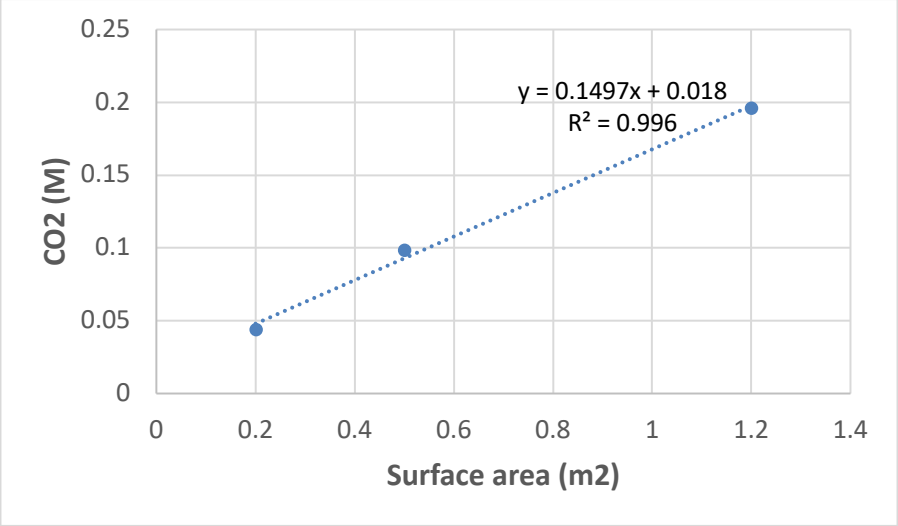

Figure 9. Initial rates of atmospheric CO_2 capture (mol/Lh) with 1 M aqueous K-SAR as a function of air–liquid contact area.

4.3. Optimization of Sorbent Regeneration and CO_2 Release

The release of the CO_2 from the MGBIG-CO_3 crystals requires heat, the amount of which is dictated by thermodynamics. The required heat for P3, measured by DSC, is 323 kJ/mol CO_2, or 7.3 GJ/ton.[6] The kinetics of CO_2 release were measured by isothermal TGA, using mg-scale samples, and were found to be very fast, typically taking a couple of minutes, at temperatures higher than 100 °C. However, when we tried to regenerate larger amounts of MGBIG (e.g., 100 g) in the oven, we found that it takes much longer, a few hours, to complete, which is probably because of the poor air to solid heat transfer. To overcome this limitation, we employed two regeneration approaches, using either microwaves or steam to provide the energy required to release the CO_2.

In the first approach, we employed a household microwave oven to regenerate MGBIG. In this approach, we took advantage of the water included in the MGBIG-CO_3 crystals, tightly bound on the carbonate anions through hydrogen bonding. We reasoned that exciting these water molecules with microwaves would deliver the heat more efficiently to the carbonate anions and release the CO_2, thereby overcoming the heat transfer limitations. We found the microwave heating released the CO_2 much more effectively than convection heating, taking about 5 min to fully release the CO_2, compared to at least 30 min with convection heating (Figure 10). The microwave regeneration scales up well – it takes less than 20 min to regenerate 50 g of MGBIG, compared to more than 2 hours by convection heating.[7]

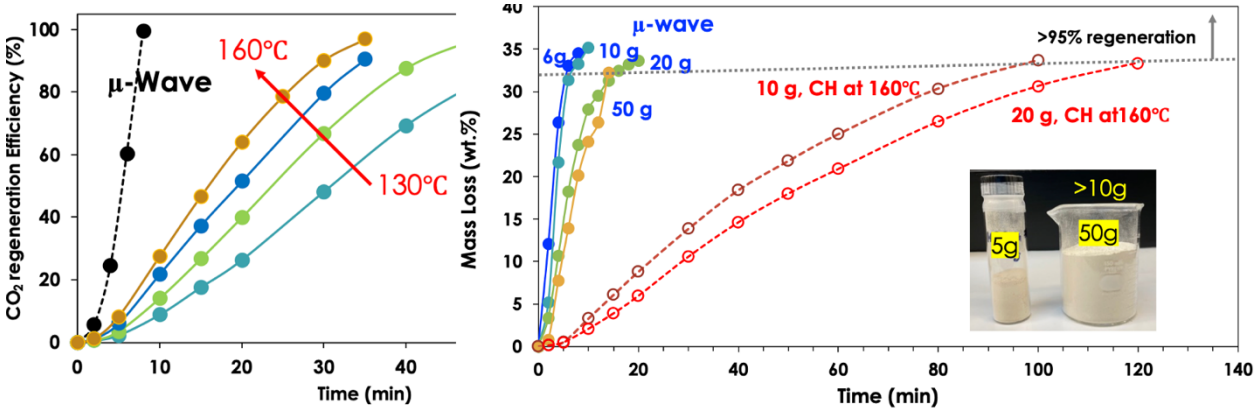

Figure 10. Regeneration of MGBIG by microwave heating, compared to convection heating.

The second regeneration approach pursued as part of this project involved direct steam heating. A steam reactor was designed for this purpose, as shown in Figure 12. The reactor has a frit for placing the MGBIG-CO_3 solid and two side tubes for delivering the steam. As CO_2 is released and some of the excess steam is condensed, the regenerated MGBIG solid is dissolved into water, and the resulting solution is collected through a bottom tube (Figure 11). Thus, direct steam heating presents a unique advantage, in that the MGBIG is regenerated as aqueous solution that can be easily recycled into the air–liquid contactor. As plotted in Figure 12, direct steam regeneration is significantly more efficient than regeneration by convection heating at temperatures between 100 and 132 °C.

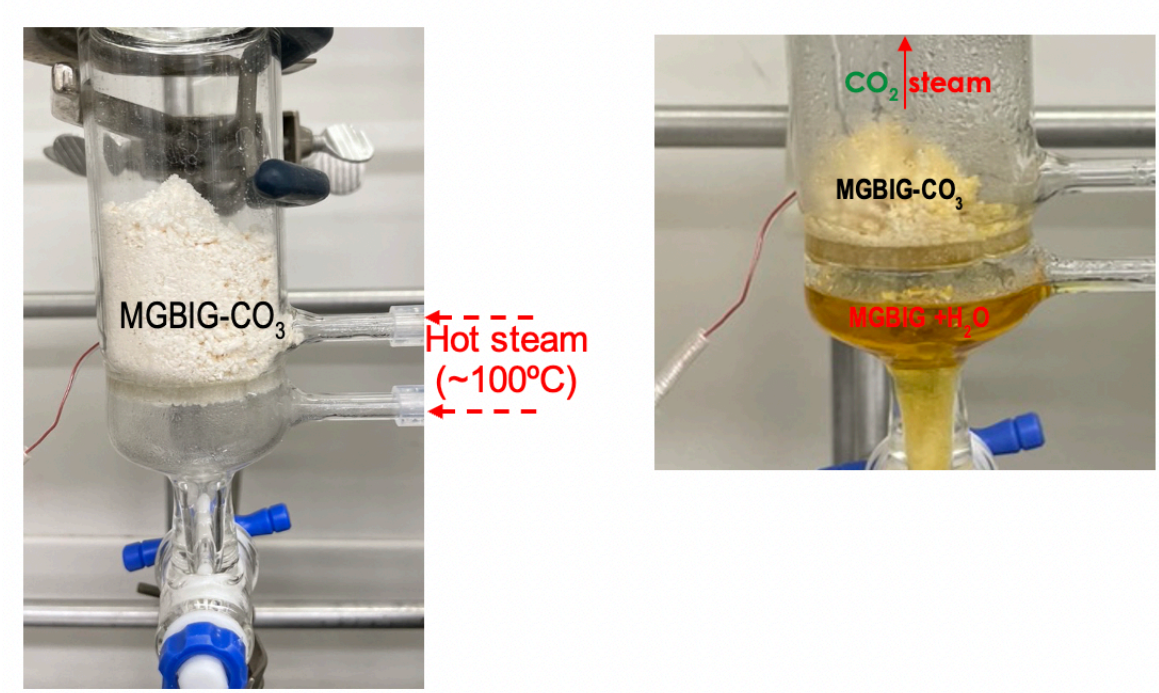

Figure 11. MGBIG regeneration by direct steam heating. The MGBIG-CO_3 (10 g) was placed on a frit inside the glass reactor, and hot steam was delivered through the side tubes. As the CO_2 is released and excess steam condenses, the regenerated MGBIG solid is dissolved into water, and the resulting solution is collected through the bottom tube.

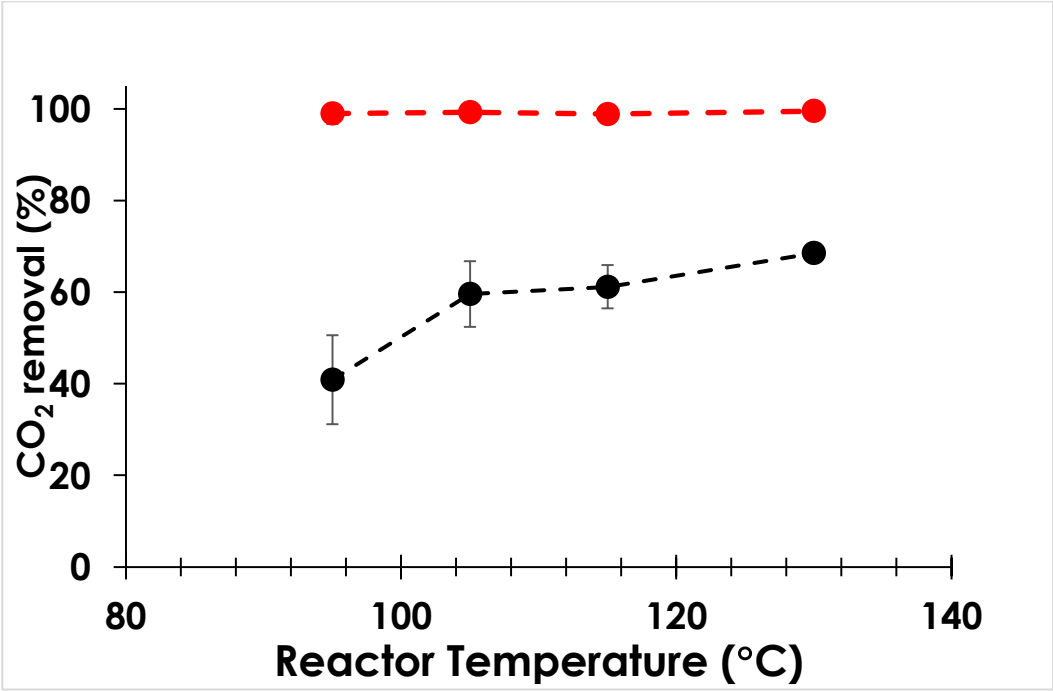

Figure 12. Comparison of regeneration by direct steam heating (red) vs convection heating (black). In all cases, the MGBIG-CO_3 (P3) solid was heated for 30 min.

4.4. DAC Process Engineering and Intensification

An intensified DAC process was designed, as shown in Figure 13. The process combines CO_2 absorption by the SAR amino acid and crystallization with MGBIG inside the RAC. The resulting MGBIG-CO_3 slurry is then pumped into a filter press that separates the solvent, which is recycled into the contactor, and the MGBIG-CO_3 carbonate solid, which is transferred to the steam reactor for regeneration. The CO_2 is released and carried away with the excess steam, which is condensed to produce pure CO_2. Finally, the aqueous MGBIG solvent is continuously returned to the contactor to capture more CO_2. Employing the 2nd gen RAC with this process, we estimate we can separate about 100 g CO_2/day.

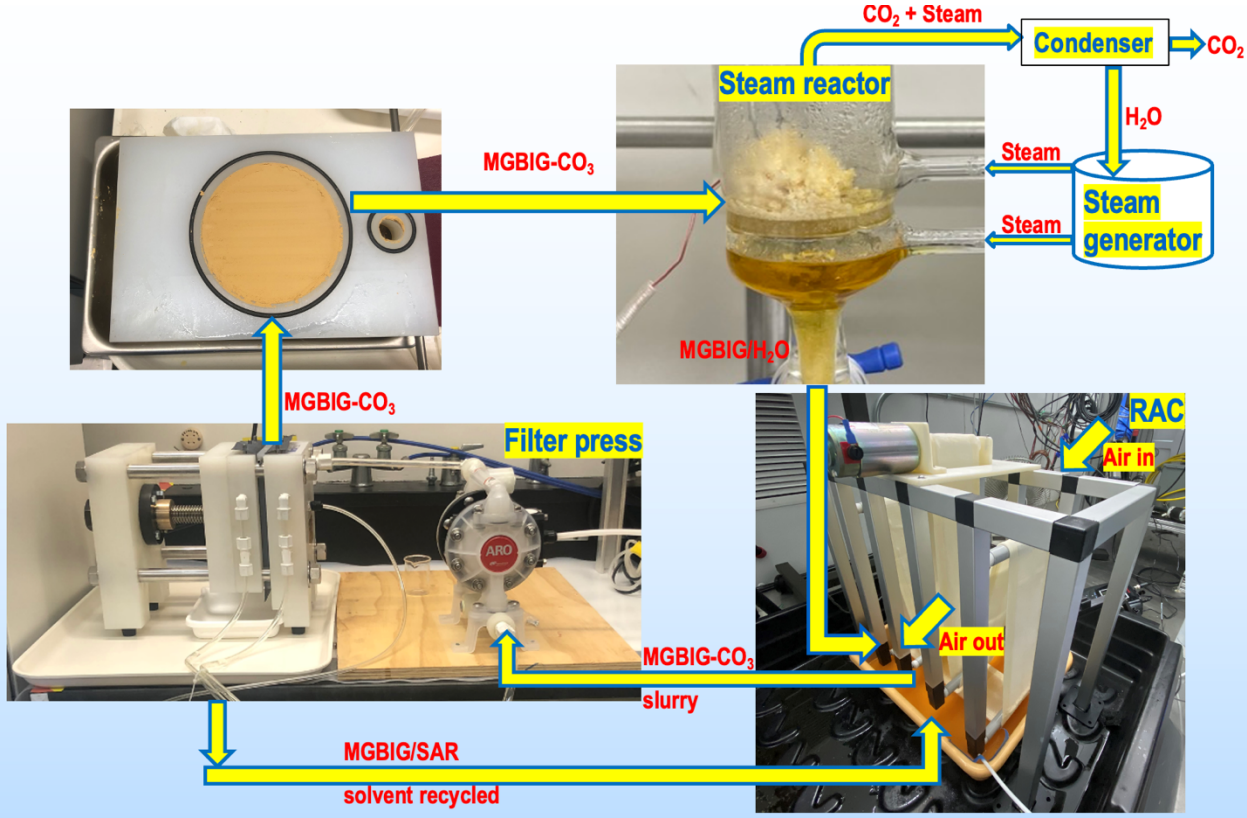

Figure 13. Intensified DAC process combining CO_2 absorption by the SAR amino acid and crystallization with MGBIG into a single stage.

4.5. Atmospheric Water Capture

Atmospheric Water capture work was performed at Reactwell's former Port Allen, LA USA site, 1441 Canal Street, Lab 301, New Orleans, LA USA as well as at the former China Lake, CA test site at Coso Geothermal Power Plant.

The laboratory work performed in New Orleans, LA USA included reviewing sorbents and absorbents for Direct Air Capture DAC of water, as well as reviewing older waste adsorbent materials from pre-existing manufacturer sites. The field scale-up work at Coso Geothermal Operating Plant, on DOD lands at Navy NAVFAC China Lake, CA USA utilized a 275-gallon tote to accumulate water through cycling the unit on a continuous basis, as well as during the

condensation window at sunset when in the desert the moisture drops out of the air and into the collection system. Our more advanced unit built was a 20-ft long module that performs vapor compression distillation on water. Coupling this with the adsorbent material enabled us to capture only water vapor with energy input and not water vapor and air, which results in excessive energy consumption. Therefore, based upon our atmospheric water capture work, strategically tied into pre-existing air flows of cooling water tower systems, resulted in a 50% water recovery. Based upon our laboratory work, assembly work and field demonstration work of various absorbent and adsorbent systems, atmospheric water recovery is not the bottleneck, but carbon dioxide capture is the limiting step. Our next step is to integrate the atmospheric water capture with carbon dioxide capture systems and a cooling water tower. To effectuate this work, our team has been collaborating with owners of a cooling water tower system in operation at Citgo Lake Charles, LA USA that utilizes a scalable and simple design.

Key information gathered and insights are as follows:

1. It is not economical to simply flow air through a condenser system 24x7 to capture the water as this results in excessive energy use by other species to flow through the system and result in parasitic losses (e.g. nitrogen, oxygen, and argon).

2. The use of a sorbent filtration system to separate the water vapor and condensate from the air (when pulled during the critical transition time from sunset to nighttime when the wet bulb shifts drastically and nature's energy change results in efficient operation) results in the best deployment of energy resources stored during the daytime sunlight or from geothermal power plant energy demands and loads at the field test site. The thermoelectric geothermal powerplant with turbine performs better at nighttime with T.c cold sink decreased in order to utilize a slipstream of power, while assisting the plant in lessening its turndown requirements as daytime loads transition to nighttime loads. Solar thermal, as well as Geothermal, direct use was also evaluated in the sorbent system regeneration and, for a site independent system, the solar thermal plastic black tube on ground provides sufficient T.h driving temperature for vacuum compression sorbent regeneration system to function properly.

4.6. Electrochemical Conversion of CO_2 to Ethanol

During the electrochemical conversion of carbon dioxide to ethanol work, utilizing the original process at ORNL did not result in synthesis of ethanol from the carbon nanospikes (CNS) substrate when doped with copper. Our team had to modify the original ORNL electrochemical reactor to convert it into a hybrid photoelectrochemical reactor design that was able to synthesize ethanol from water, but only when the gas phase side of the hybrid photoelectrochemical reactor had no water vapor present.[8] When we fed saturated water, via bubbler to the gas phase side of the photoelectrochemical reactor with no coherent laser on the electrode, it would quench and stop the ethanol synthesis reaction. However, when we fed carbon dioxide gas (dry) to the gas phase side of the hybrid photoelectrochemical reactor, ethanol synthesis would immediately start. Our work was published in American Chemical Society ACS as well as Royal Chemical Society RCS regarding the working and replicable photoelectrochemical reaction utilizing carbon nanospike CNS catalyst system (Figure 14).

Hybrid gas/liquid-fed electrochemical flow reactors may become attractive alternatives for chemical synthesis once it is understood how catalytic product selectivity may be optimized through the control of gas phase reactants. Using a constant pH basic electrolyte to suppress the hydrogen evolution reaction, we explore how protonation by water vapor added to the flowing CO_2 supply affects the CO_2 reduction reaction. Although H_2 remains the dominant product, supplying dry CO_2 gas selectively produces more C_2 products than C_1. However, adding protons through water vapor changes selectivity toward C_1 products, increasing the overall faradaic efficiency of hydrocarbon production while reducing H_2 production.

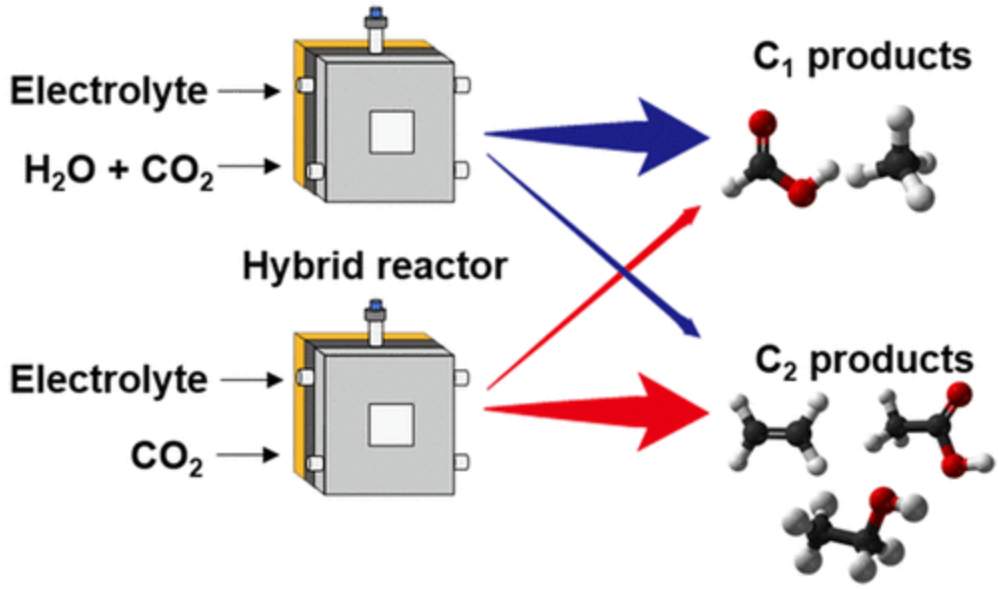

Figure 14. Electrochemical conversion of CO_2 into ethanol and other C_1 and C_2 products.

For the conversion of CO_2 into fuels and chemical feedstocks, hybrid gas/liquid-fed electrochemical flow reactors provide advantages in selectivity and production rates over traditional liquid phase reactors. However, fundamental questions remain about how to optimize conditions to produce desired products. Using an alkaline electrolyte to suppress hydrogen formation and a gas diffusion electrode catalyst composed of copper nanoparticles on carbon nanospikes, we investigated how hydrocarbon product selectivity in the CO_2 reduction reaction in hybrid reactors depends on three experimentally controllable parameters: (1) supply of dry or humidified CO_2 gas, (2) applied potential, and (3) electrolyte temperature (Figure 15). Changing from dry to humidified CO_2 dramatically alters product selectivity from C_2 products ethanol and acetic acid to ethylene and C_1 products formic acid and methane. Water vapor evidently influences product selectivity of reactions that occur on the gas-facing side of the catalyst by adding a source of protons that alters reaction pathways and intermediates.[8]

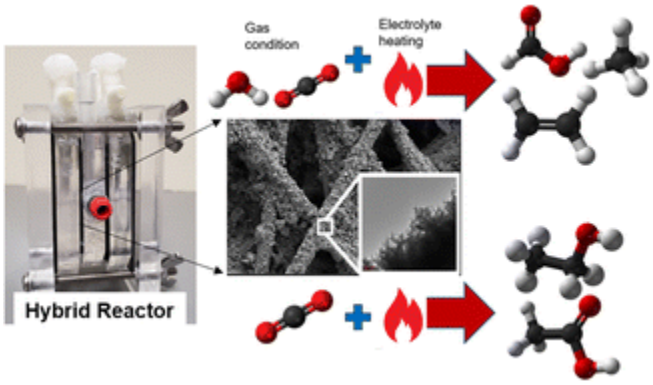

Figure 15. Controlling the hydrocarbon product selectivity in the CO_2 reduction reaction in hybrid reactors.

4.6. Technoeconomic Analysis

A technoeconomic assessment (TEA) of the intensified DAC process involving SAR and MGBIG was performed as part of this project. This TEA is for a stand-alone DAC plant working at a CO_2 removal capacity of 1 MM t CO_2/year. It does not include the electrochemical conversion to ethanol, which requires further optimization before it can be scaled up and commercialized.

Methodology and key assumptions. The process model of the intensified phase-change DAC using MGBIG + SAR solvent was conceptually developed in a commercial process simulation tool ASPEN Plus V12.1[9]. The process simulation, mass and energy balance and equipment design were performed base on 1 MM tonne CO_2 captured per year, which is comparable to the scale designed by Carbon Engineering (CE)[10]. Financial assumptions used in this cost analysis are consistent with U.S. DOE's analysis works [11] in which the "n^{th}" plant assumptions are used. This analysis work does not account for additional first-of-a-kind plant costs, including special financing, equipment redundancies, large contingencies, and longer startup times necessary for the first few plants. All costs in this work are presented in a 2020 constant US dollar basis.

A simple process block flow diagram to capture CO_2 by using MGBIG + SAR solution is shown in Figure 16. Most of basic equipment such as pump, compressor, flash tank, heat exchanger were manually designed and sized before ASPEN Economic Evaluation tool[9] was applied to estimate the equipment costs. For special design equipment such as air contactor and the MGBIG catalyst regeneration system, the equipment design and costs published in research literature were used. The air contactor design, cost, and energy consumption are comparable to the data reported by CE[12]. The MGBIG regeneration system is assumed to be similar to commercial slurry drying conveyor unit[13] where the slurry was warmed/heated up and filtered along the conveyor belts. Heat integration was performed in the process model to minimize heat loss and maximize the overall process efficiency. The catalyst regeneration step is carried out at 100 °C which can be done by using low pressure steam. This low temperature guanidine regeneration method allows the process to be electrified. A commercial mechanical vapor recompression (MVP) system is assumed to produce steam from electricity. Low pressure steam from the MVP unit is used to supply heat and release CO_2 from MGBIG-carbonate. The design, cost, and energy consumption of the MVP system can be found elsewhere [14, 15].

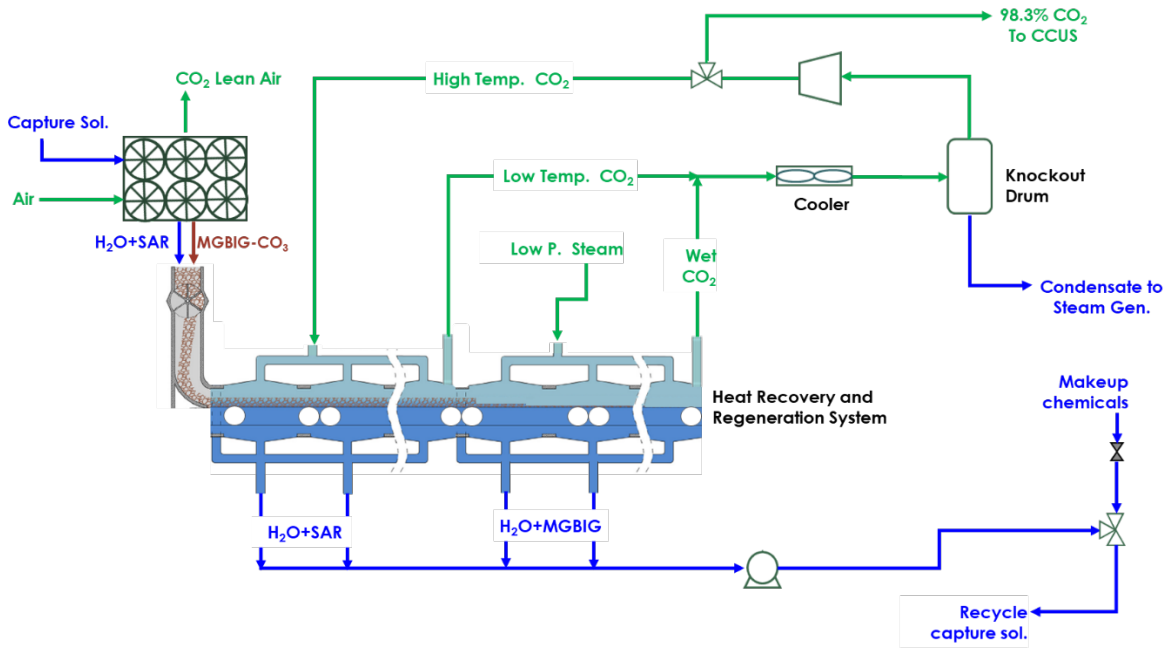

Figure 16. Block flow diagram of DAC process with MGBIG + SAR solvent.

Preliminary cost estimation for the base case. The base case analysis adopted a CO_2 capture efficiency of 75% and a chemical loss rate of 0.5% (both MGBIG and SAR) per year. Cash flow calculation suggested that install capital cost and total of project investment are approximately MM$ 510 and MM$ 720, respectively. Cost of CO_2 capture is approximately $280/tonne CO_2 when 50% of the total cost is capital related and 34% of the total cost is chemical cost (MGBIG and SAR). Electricity cost is less than 15% of the CO_2 capture cost and labor cost is an insignificant cost driver.

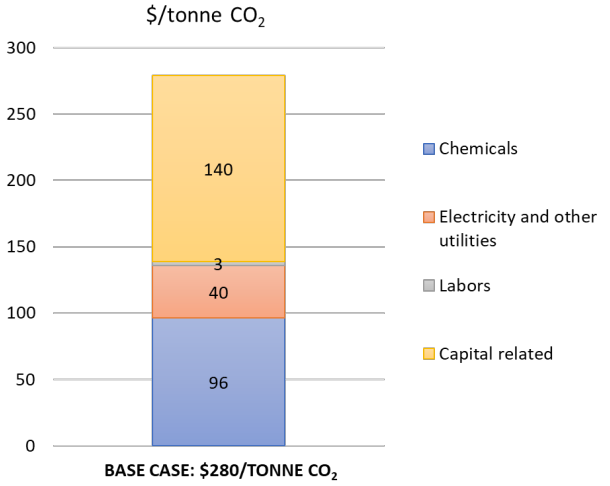

Figure 17. Base case cost estimation for the intensified phase-change DAC using MGBIG + SAR solvent.

Sensitivity analysis and pathway to $100/tonne CO_2. Process performance and cost components driving the CO_2 capture cost include time on stream, CO_2 capture efficiency, utility cost, chemicals

makeup, and capital cost. Sensitivity to these parameters towards reaching \$100/CO_2 is presented in Table 2 and Figure 18. Time on stream used in the base case study is 85% (7,446 hours/year). The process economics can be improved by \$16/tonne CO_2 if the plant is operated at 95% time on stream (8,322 hours/year). The capture efficiency in the base case is at 75% (comparable to CE process) and the cost can be significantly improved by \$101/tonne CO_2 with a CO_2 capture efficiency of 95%. Grid electricity cost of 7 cents/kWh is used in the base case. Inexpensive electricity cost of 2 cents/kWh (future target cost suggested in previous US DOE's work)[3] could reduce the capture cost by \$30/tonne CO_2. The chemicals cost is one of the most significant operating costs. MGBIG and SAR costs are assumed at \$1.4/kg and \$0.4/kg, respectively in the base case. Reducing the chemicals replacement from 0.5% to 0.1% per year will reduce the cost by \$79/tonne CO_2. In addition to the operating cost, 50% of CO_2 capture cost is capital related (Figure 18). The sensitivity study shows that CO_2 capture cost can be reduced by \$60/tonne CO_2 if the project investment can be reduced by 50%. To achieve \$100/tonne CO_2 capture cost, improvements in multiple cost components are necessary.

Table 2. Possible DAC process improvements to achieve \$100/t CO_2.

Sensitivity to:	**\$/tonne CO_2**	**Cost improvement (compared to base case @\$280/tonne CO_2)**
Time on Stream, 95% (vs 85%)	264	16
Capture efficiency, 85% (vs 75%)	209	71
Capture efficiency, 95% (vs 75%)	179	101
Electricity cost, 2 cents/kWh (vs 7 cents/kWh)	250	30
Chemicals makeup, 0.1% (vs 0.5%)	201	79
Total project investment, –50%	220	60

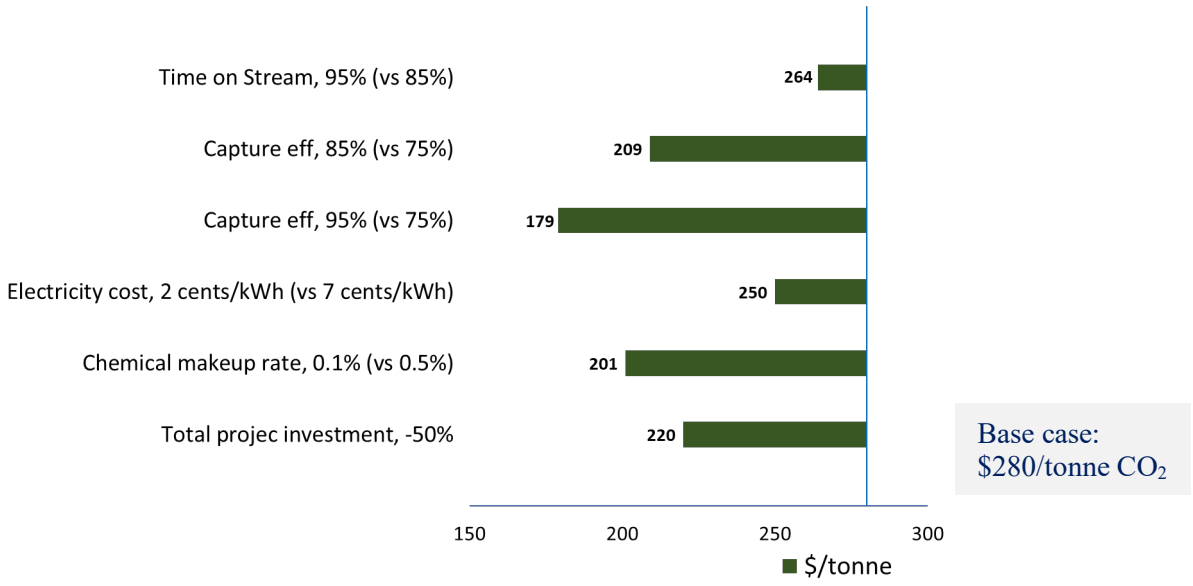

Figure 18. CO_2 capture cost reduction from operating and capital cost improvements.

5. Subject Inventions

Three ORNL invention disclosures have been submitted as part of this CRADA:

1. Microwave Regeneration of Water-lean Solvents and Sorbents Used for CO_2 Capture. ID# 81938781. Non-provisional patent application: Microwave Regeneration of Carbon Dioxide Sorbents; Patent ID – 81944506; App. No. 18/235,081.

2. DSR (Direct-steam Sorbent Regeneration). ID# 202305436. Provisional patent application: Methods of Energy Efficient Sorbent Regeneration Used for Direct Air Capture; Patent ID – 81947812; App. No. 63/534,893.

3. Direct Air Capture of CO_2 Using RAC (Rotating Air Contactor). ID# 81946146. Provisional patent application: Rotating Air Contactor for Direct Air Capture of CO_2; Patent ID – 81948020; App. No. 63/535,383.

6. Commercialization Possibilities

Reactwell is building a facility for scale-up of their CO_2 electrochemical conversion to ethanol. Toward this goal, they will continue working with China Lake, CA Navy NAVFAC's geothermal power plant on-site.

ORNL has also licensed their DAC chemistry to Holocene Climate Corporation (HCC). HCC plans to scale up the DAC process with amino acids + guanidines to 10 t CO_2 removal per year by the end of 2024.

7. Plans for Future Collaboration

ORNL started a collaboration with HCC on process development and scaleup of the MGBIG/SAR DAC technology.

8. Conclusions

This CRADA facilitated the development of a DAC technology involving atmospheric CO_2 removal followed by its electrochemical conversion to ethanol through a collaboration between ORNL and Reactwell. A continuous intensified DAC process employing aqueous amino acids/guanidines solvents was developed at ORNL at a scale of 100 g CO_2 removed per day. The TRL of this technology was advanced from 3 to 4. While the initial plan was to develop a combined process that integrates DAC with CO_2 conversion, at the end of the project we concluded that a standalone DAC process has its own merits. Specifically, a DAC process independent of CO_2 conversion has the potential to become carbon negative if coupled with CO_2 storage. Another advantage of a standalone DAC process is that the scales and the rates of the DAC and conversion do not necessarily have to be matched. Thus, the DAC process could be scaled up to a much larger scale, of 1 MM t CO_2/year or larger, with only a fraction of the CO_2 converted to products, and the bulk of CO_2 sent to permanent storage. Furthermore, the CO_2 removed from air could be stored temporarily as BIG-carbonate solid, and transported to a different location where it can be released

on demand for conversion into ethanol or other products. This would allow the technology to achieve negative emission status, while generating a profit through commercialization of the ethanol. Moving forward, both options, the standalone DAC and the integrated DAC with conversion to ethanol or other products will be further explored for commercialization, in collaborations with HCC and Reactwell, respectively.

8. References

[1] Custelcean, R. *Iminoguanidines: From Anion Recognition and Separation to Carbon Capture, Chem. Commun.* **2020**, *56*, 10272-10280.

[2] Custelcean, R. *Direct Air Capture of CO_2 via Crystal Engineering*, *Chem. Sci.* **2021**, *12*, 12518-12528.

[3] Custelcean, R. *Direct Air Capture with Bis-iminoguanidines: From Discovery to Commercialization, Chem* **2021**, *7*, 2848-2852.

[4] Custelcean, R.; Williams, N. J.; Wang, X.; Garrabrant, K. A.; Martin, H. J.; Kidder, M. K.; Ivanov, A. S.; Bryantsev, V. S. *Dialing in Direct Air Capture of CO_2 by Crystal Engineering of Bis-iminoguanidines, ChemSusChem,* **2020**, *13*, 6381-6390.

[5] Stamberga, D.; Thiele, N. A.; Custelcean, R. *Synergistic Direct Air Capture of CO_2 with Aqueous Guanidine/Amino Acid Solvents, MRS Advances* **2022**, *7*, 399-403.

[6] Kasturi, A.; Jang, G. G.; Stamberga, D.; Custelcean, R.; Yiacoumi, S.; Tsouris, C. *Determination of the Regeneration Energy of Direct Air Capture Solvents/Sorbents Using Calorimetric Methods, Separation and Purification Technology* **2023**, *310*, 123154.

[7] Jang, G. G.; Kasturi, A.; Stamberga, D.; Custelcean, R.; Keum, J. K. Yiacoumi, S.; Tsouris, C. *Ultra-fast Microwave Regeneration of CO_2 Solid Sorbents for Energy-Efficient Direct Air Capture, Separation and Purification Technology* **2023**, *309*, 123053.

[8]. Lee, H.S.; Song, Y.; Iglesias, B.; Everitt, H. O.; Liu, J. *ACS Appl. Energy Mater.* 2022, 5, 8, 9309.

[9] https://www.aspentech.com/en/products/engineering/aspen-plus

[10] https://doi.org/10.1016/j.joule.2018.05.006

[11] https://www.energy.gov/eere/vehicles/articles/us-drive-net-zero-carbon-fuels-technical-team-analysis-summary-report-2021

[12] https://doi.org/10.1098/rsta.2012.0137

[13] https://inldigitallibrary.inl.gov/sites/sti/sti/6359707.pdf

[14] https://www.powerengineeringint.com/renewables/steaming-ahead-with-mvr/

[15] https://genless.govt.nz/assets/Business-Resources/Mechanical-vapour-recompression-for-evaporation-distillation-drying.pdf